Supporting Information

KNO_3-assisted incorporation of K dopants and N defects into g-C_3N_4 with enhanced visible light driven photocatalytic H_2O_2 production

Haihua Yang,[a,b] Xiaorong Qian,[a,b] Na Zhang,[c] Li Zhang,[a,b] and Minjie Zhou [*a,b]

[a] *Key Laboratory of Hunan Province for Advanced Carbon-Based Functional Materials, Hunan Institute of Science and Technology, Yueyang, Hunan Province, 414006, P.R. China*

[b] *School of Chemistry and Chemical Engineering, Hunan Institute of Science and Technology, Yueyang, Hunan Province, 414006, P.R. China*

[c] *School of Physics and Electronic Science, Hunan Institute of Science and Technology, Yueyang, Hunan Province, 414006, P.R. China*

[*]Corresponding Author. E-mail: zmj0104@163.com

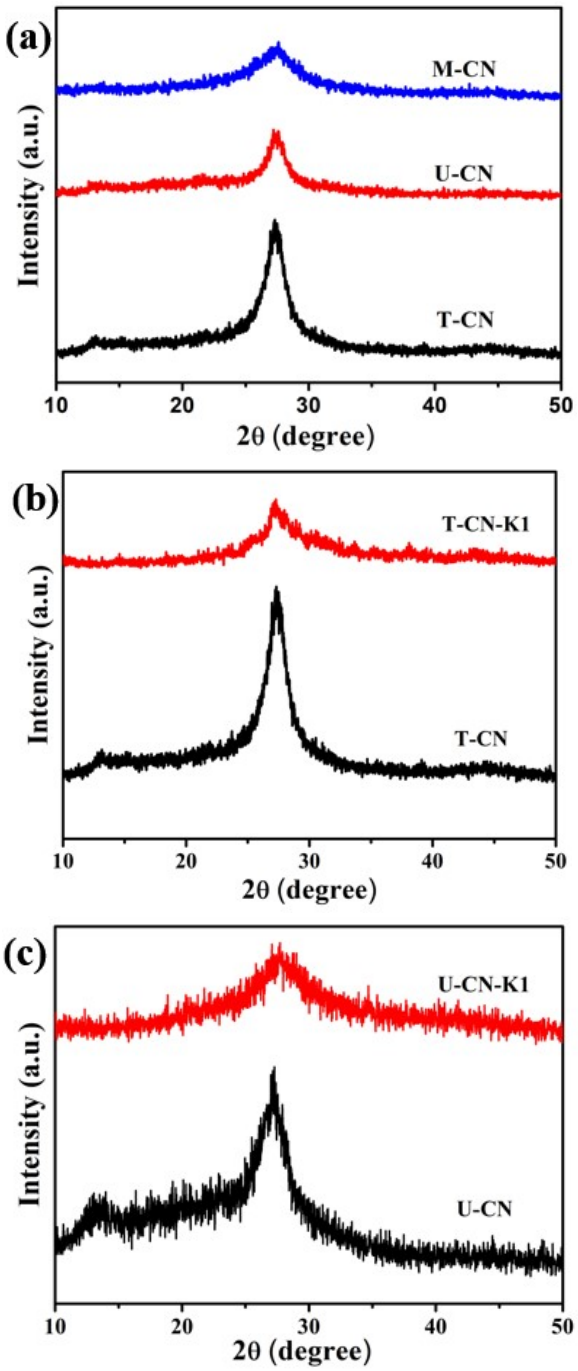

Figure S1. XRD patterns of the pristine and modified g-C_3N_4 samples.

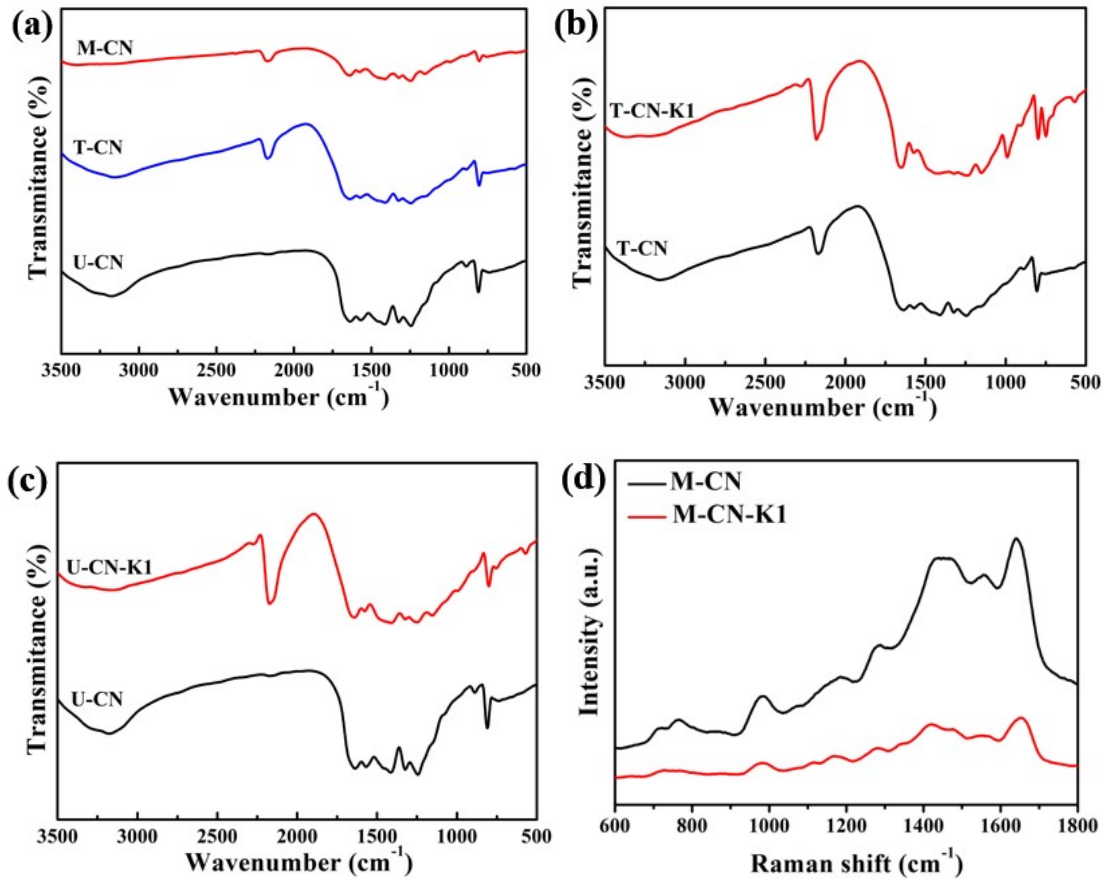

Figure S2. (a-c) FT-IR spectra and Raman spectra (d) of the pristine and modified g-C_3N_4 samples.

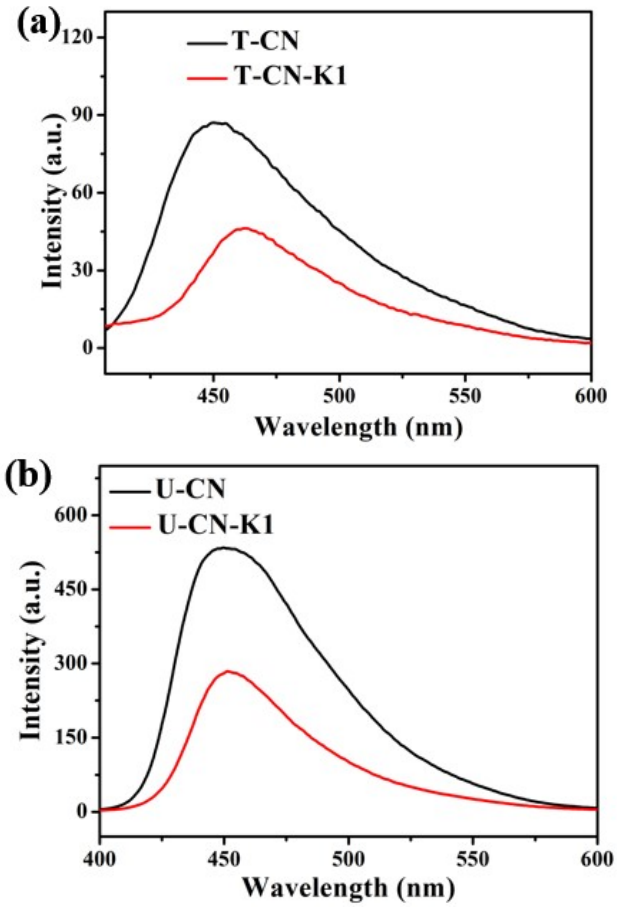

Fig. S3. Steady-state PL emission spectra of the pristine CN and CN-K1.

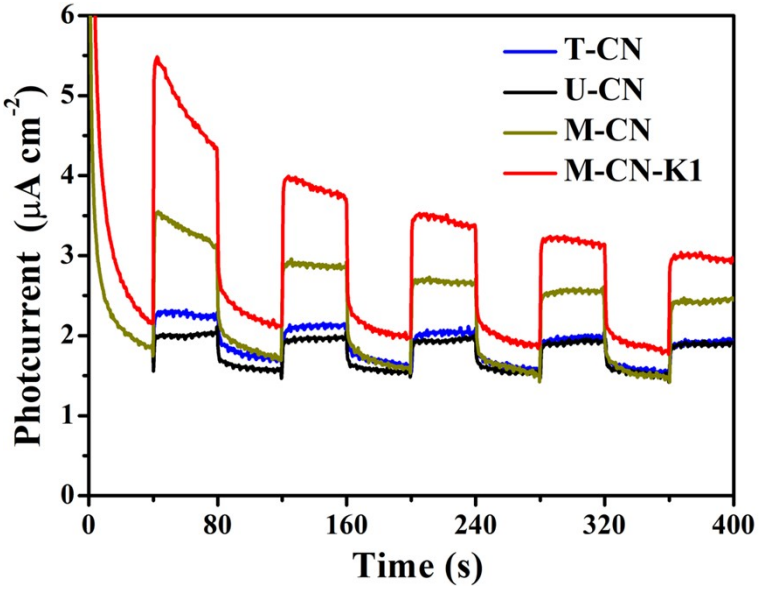

Fig. S4. Photocurrent responses of pristine and modified g-C_3N_4 photocatalysts.

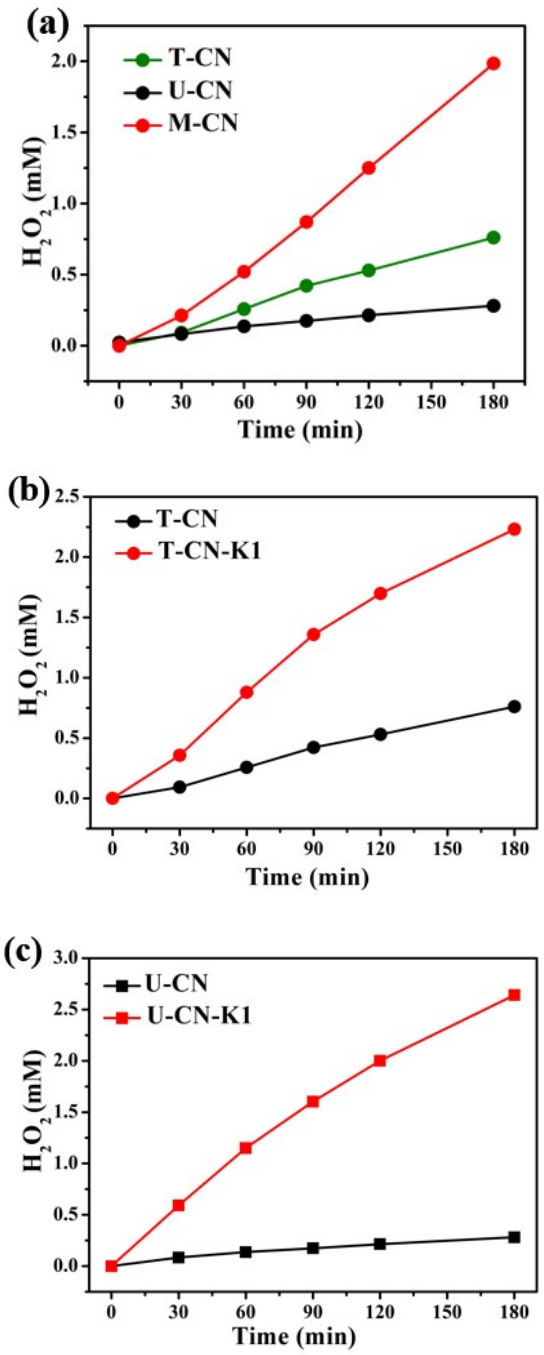

Fig. S5. Time profiles of photocatalytic H_2O_2 production by pristine and modified g-C_3N_4 photocatalysts under visible light irradiation.

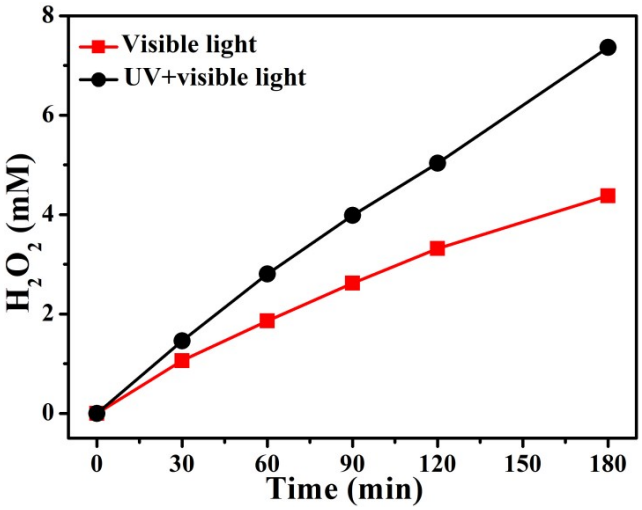

Fig. S6. Comparison of photocatalytic H_2O_2 production by M-CN-K1 under UV+visible and visible light irradiation, respectively.

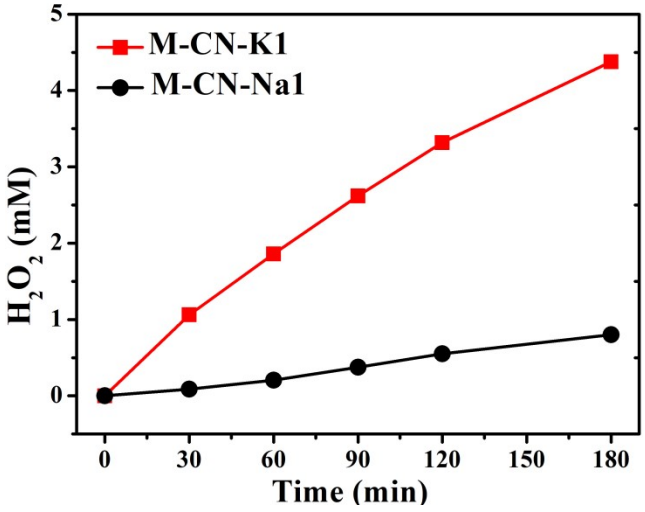

Fig. S7. Comparison of visible light driven photocatalytic H_2O_2 production by M-CN-K1 and M-CN-Na1, respectively.

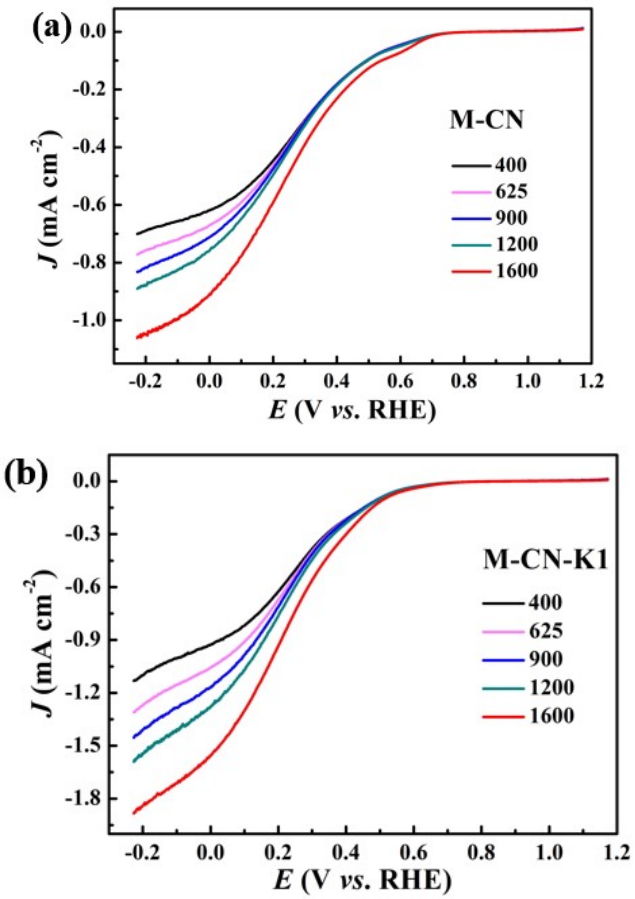

Fig. S8. LSV curves of M-CN (a) and M-CN-K1 (b) measured on RDE at different rotating speeds.

Table S1. Elemental composition of M-CN and M-CN-K1

Catalyst	C (at %)	N (at %)	K (at %)	O (at %)
M-CN	42.1	53.3	0	4.6
M-CN-K1	43.6	51.1	1.1	4.2